Journal of Applied Physics ARTICLE scitation.org/journal/jap

Time response of spin-polarized rubidium thermal gas with radio-frequency pulse driving

Cite as: J. Appl. Phys. **131**, 134402 (2022); doi: 10.1063/5.0082535
Submitted: 16 December 2021 · Accepted: 18 March 2022 ·
Published Online: 4 April 2022

Yanhua Wang,[1,2,3,a)] Zhihua Kang,[1] Li Yang,[1] Qiang Ma,[1] Yu Wang,[1] Yabin Dong,[1] and Junmin Wang[2,3,b)]

AFFILIATIONS

[1]School of Physics and Electronic Engineering, Shanxi University, Taiyuan, Shanxi 030006, China
[2]State Key Laboratory of Quantum Optics and Quantum Optics Devices, and Institute of Opto-Electronics, Shanxi University, Taiyuan, Shanxi 030006, China
[3]Collaborative Innovation Center of Extreme Optics, Shanxi University, Taiyuan, Shanxi 030006, China

[a)]**Author to whom correspondence should be addressed:** wangyanhua@sxu.edu.cn
[b)]**Electronic mail:** wwjjmm@sxu.edu.cn

ABSTRACT

The time evolution of the polarization of a rubidium atom spin ensemble driven by a resonant radio-frequency (RF) magnetic field is analyzed based on the rate equation. A simple optical pumping experimental system is constructed and the time response of the rubidium atomic ensemble is demonstrated by recording the transmitted intensity of pumping light. In the steady-state response, the polarization difference between the optical pumping steady state and the magnetic resonance steady state depends on the optical pumping power and RF magnetic intensity. We can obtain the optimal power value corresponding to the maximum polarization difference. In terms of transient response, where the intensity of RF magnetic field is too weak to observe Rabi oscillations, two decay processes between magnetic resonance and optical pumping steady states are monitored. The decay time from magnetic resonance steady state to optical pumping steady state depends on the optical pumping rate and the spin relaxation rate. The decay time from optical pumping steady state to magnetic resonance steady state depends on the optical pumping rate, the RF driving rate, and the spin relaxation rate. The scale factor of pumping rate to pumping power is obtained, in addition to that of RF driving rate to the RF magnetic field. It can provide an intuitive understanding of the spin dynamic evolution of the polarized atomic ensemble.

I. INTRODUCTION

The spin-polarized thermal alkali gas cell is the basic component in the service of precision measurement and quantum sensor,[1] from atomic frequency standard[2] atomic magnetometers[3,4] to the nuclear magnetic resonance (MR) co-magnetometer.[5] It paves the way for highly sensitive applications, including magnetoencephalography (MEG)[6,7] and magnetocardiography (MCG),[8,9] geophysical exploration, material defect imaging,[10] electric dipole moment measurement (EDM),[11] and spin-based amplifiers for dark matter searching.[12,13] Furthermore, the process of spin exchange optical pumping, based on the spin-polarized alkali atoms, can realize the hyper-polarization of noble gas,[14,15] and it expends the application fields to magnetic resonance imaging for medical diagnosis[16] and quantum gyroscopes for high-precision navigation.[17] In addition, a neutron spin filter can be realized based on the polarization of ^{3}He.[18]

Optical pumping,[19,20] in particular, is a preferred choice to polarize alkali atoms and attain the macroscopic magnetic moment, in which the circularly polarized pumping light transfers angular momentum to the atomic ensemble. Subsequently, the magnetic moment undergoes Larmor spin precession in a magnetic field. In detail, the spin precession accompanies relaxation due to thermal motion collision and spatial uniformity. The complicated relaxation mechanisms are presented as wall collision, spin exchange, and spin destruction. In order to suppress the relaxation processes, buffer gas is often introduced to slow down the collision and diffusion motion of polarized atoms. Another approach is to coat the internal wall with antirelaxation film such as paraffin[21,22] or octadecyltrichlorosilane.[23,24]

Moreover, it is an important topic to characterize the spin evolution. Generally, passing through the spin-polarized gas ensemble, the deflection angle of polarization plane for the linearly

polarized probe laser can be used to characterize the frequency or the phase of the precession process, in addition to the magnitude of the polarized magnetic moment. In addition, the absorption or transmitted intensity of the pumping laser also carries the information of the polarization and spin evolution.[25,26] Combining the information of the deflection angle of probe and transmitted intensity of pumping, the three-axis magnetometer[27,28] can be demonstrated.

The time dependent response of spin is a traditional topic. Some experimental methods, such as free induction decay (FID)[29] and spin echo,[30] are utilized to monitor the spin evolution. Recently, the diffusion effect of the warm atomic ensemble is described by the Bloch–Heisenberg–Langevin formalism, the spin noise spectrum, squeezed spin state lifetime, and coherent coupling are calculated.[31] The dynamic response of spin precession in a time dependent magnetic field is studied.[32,33] With a square-wave switched main magnetic field in the spin-exchange-relaxation-free regime[34] and with a radio-frequency (RF) field controlling, the transient evolution of the magnetic resonance with Rabi oscillation is demonstrated experimentally.[35]

However, it is absent for the time response of the polarized ensemble driven by a weak RF. In this paper, the time response analysis is provided. Using the rate equation formalism, we analyze two polarization steady states and the evolutionary processes between them, where the polarization steady states are switched by the RF pulse. We use a simple experimental apparatus to record the polarization of an atomic system. The real-time polarization information is extracted from the transmitted intensity of the pumping laser.

This paper is organized as follows. In Sec. II, the experimental apparatus is briefly described. In Sec. III, the process of atomic spin polarization is theoretically analyzed based on the rate equation. In Sec. IV, the steady-state response of polarization is studied theoretically and experimentally. In Sec. V, the transient response of an atomic spin system driven by an RF pulse is analyzed.

II. EXPERIMENTAL SETUP

Figure 1 shows the experimental setup. A spherical gas cell of about 50 mm in diameter is filled with natural rubidium and almost 160 Torr nitrogen. The Helmholtz coils in the x and y directions are employed to compensate the residual transverse magnetic fields. There are two pairs of Helmholtz coils in the z direction, driven by two constant current sources separately. One provides the DC bias magnetic field to compensate the longitudinal residual fields and provide the main field in the z direction around 20 000 nT, and the other is used to scan the z direction field and search for the condition of magnetic resonance. A pair of RF coils are placed in the y direction symmetrically, which maintains the magnetic resonance (about 94 kHz) with the applied magnetic field along the z direction. The voltage controlled constant current source CS580 (Stanford Research Systems) as the driver of RF coils is controlled with an RF pulse, which is generated by a function generator DS345 (Stanford Research Systems). Its conversion relationship between RF magnetic field and current is about 52 nT/mA. The rubidium cell and RF coils in y axis are housed in a cylindrical oven, which is controlled to 55 °C.

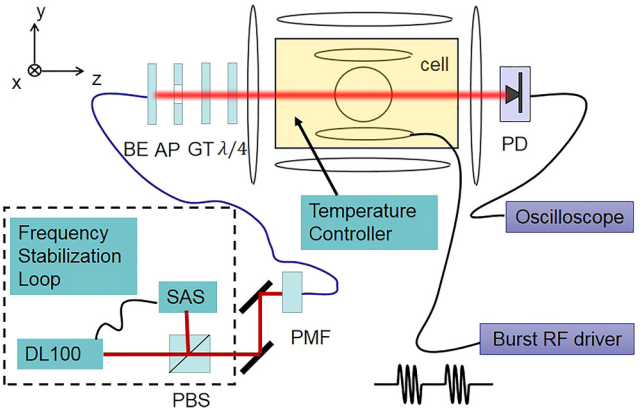

FIG. 1. A schematic diagram of the experimental setup. SAS, the Saturated Absorption Spectroscopy unit; PMF, Polarization-Maintaining Fiber; BE, Beam Expander; AP, Aperture; GT, Glan–Taylor Polarizer; $\lambda/4$, Quarter-wave Plate; PD, Photodetector; PBS, Polarization Beam Splitter.

The 795 nm laser from an external-cavity diode laser (ECDL) DL100 (Toptica Photonics) is divided into two beams. One is for laser frequency locking to the hyperfine transition F = 3 to F = 2 of rubidium 85 atoms with the saturation absorption spectrum, which is closest to the center frequency of the absorption spectrum of the thermal gas cell. The other through the polarization-maintaining fiber is transformed to circular polarization with Glan-Taylor polarizer and a quarter-wave plate, which is used to polarize the rubidium atoms and monitor the polarization as a probe. The transmitted light is detected by a photodiode. The detected signal is displayed and collected with an oscilloscope.

Experimentally, the pumping beam is expanded to about 12 mm in diameter; before the gas cell, an aperture served as the spatial filtering is added, by which the influence due to the uniformity of light intensity spatial distribution is improved. Combining the requirements of steady-state observation and multiple relaxation processes acquisition, the frequency of switching is 1 Hz. The complete switching time of the RF field is less than 1 μs.

III. ANALYSIS OF SPIN POLARIZATION PROCESS BASED ON RATE EQUATIONS

Figure 2 shows the D1 line polarization model with buffer and quenching gases for alkali metal atoms. There are two ground states 1 and 2 and two excited states 3 and 4, where N_1, N_2, N_3, and N_4 denote the population number density of atoms. Employing a circularly polarized pumping light, the atoms in state 1 are pumped to state 4 with a rate of $2R_{op}$. Due to the presence of buffer and quenching gases, the atoms in the excited states will undergo collisional mixing and decay to two ground states with equally nonradiative transition rates $S_{e1} = S_{e2}$. The rate of number density for mixed excited states $N_e = N_3 + N_4$ is

$$\frac{dN_e}{dt} = 2R_{op}N_1 - N_e(S_{e1} + S_{e2}). \quad (1)$$

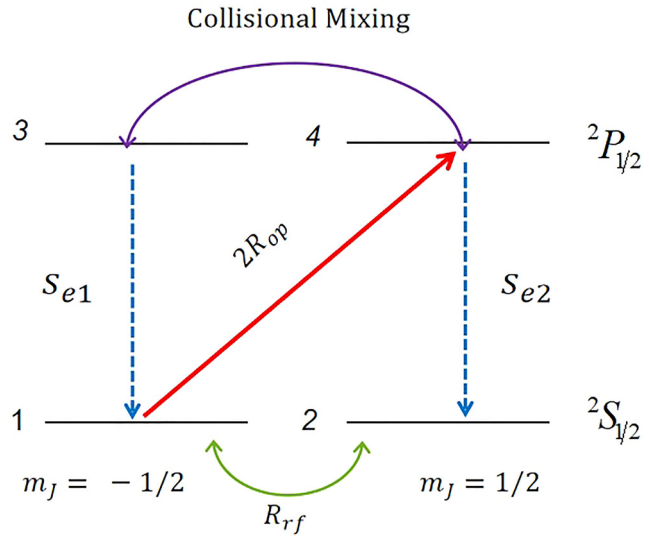

FIG. 2. D1 line polarization model for the alkali vapor with buffer and quenching gases in the cell. $2R_{op}$ is the pumping rate for circularly polarized light. R_{rf} is the driving rate of the RF field.

In consideration of $S_{e1}, S_{e2} \gg R_{op}$, Eq. (1) is always in the steady state, so it is given that $N_e(S_{e1} + S_{e2}) = 2R_{op}N_1$, and $N_e \approx 0$. The atoms are fully in the ground state. That is to say, the total number $N_{total} = N_1 + N_2 + N_3 + N_4 \approx N_1 + N_2$. So, the normalized atomic number density satisfies $n_1 + n_2 \approx 1$ ($n_i = N_i/N_{total}$).

The spin polarization of the atomic ensemble can be defined as $\langle S_z \rangle = 1/2(n_2 - n_1)$. The electron polarization is $P = |2\langle S_z \rangle|$. The rate of $\langle S_z \rangle$ is given as

$$\frac{d\langle S_z \rangle}{dt} = \frac{1}{2} R_{op}(1 - 2\langle S_z \rangle) - (2R_{rf} + R_{rel})\langle S_z \rangle. \tag{2}$$

The first term on the right-hand side of Eq. (2) is the optical pumping process. The second term is the transition process due to the RF field and the spin relaxation process. R_{rf} describes the interaction between the RF field and atoms, which depends on the detuning relative to the Lamor precession frequency and the intensity.

For the starting condition of S_0, in the presence and absence of an RF field, the electron polarization P is, respectively, expressed as

$$P = P_{MR}\left[1 - \left(1 - \frac{2S_0}{P_{MR}}\right) e^{-(R_{op}+2R_{rf}+R_{rel})t}\right] \tag{3}$$

and

$$P = P_{op}\left[1 - \left(1 - \frac{2S_0}{P_{op}}\right) e^{-(R_{op}+R_{rel})t}\right], \tag{4}$$

where

$$P_{MR} = \frac{R_{op}}{R_{op} + R_{rel} + 2R_{rf}} \tag{5}$$

and

$$P_{OP} = \frac{R_{op}}{R_{op} + R_{rel}}. \tag{6}$$

Obviously, the polarization of the atomic ensemble decays exponentially. There are two steady states for the electron polarizations P_{MR} and P_{OP}, corresponding to the magnetic resonance and optical pumping, respectively. More importantly, the polarization of the atomic ensemble can be manipulated with an RF pulse.

IV. THE STEADY-STATE RESPONSE OF POLARIZED SYSTEM

The time response of the spin-polarized system includes steady-state and transient processes. In this section, we focus on the steady-state analysis. First, the atomic system is polarized under the action of pumping light and reaches an optical pumping (*OP*) steady state, where the polarization is represented by P_{OP}. Second, when the resonant RF field is applied to the atomic system, the previous optical pumping polarization state is destroyed to some extent and a new magnetic resonance (*MR*) steady state is gradually established. At that time, the polarization is expressed by P_{MR}.

To calibrate the electron polarization in steady state experimentally, the attenuation due to optical transmission loss and absorption of the pumping laser should be mentioned. In general, the absorption of incident light depends on the atomic spin polarization and the polarization state of photons.

If the pumping laser with intensity I_{in} passes through a rubidium vapor cell, the output intensity is given as $I_{out} = I_{in}\, e^{-OD(1-sP)}$, where s is the polarization of laser and *OD* describes the optical depth. The *OD* depends on the atomic number density, the size of a cell, and absorption cross section. The circularly polarized pumping laser through the vapor cell ($s = 1$) is incident on the detector, and the output is given as $V_{out} = KI_{in}e^{-OD(1-P)}$, where the K represents the conversion coefficient between light intensity and voltage. With a fully polarized ensemble $\langle S_z \rangle = 1/2$ and $P = 1$, the absorption of circularly polarized pumping laser disappears and the maximum output voltage is attained as $V_{max} = KI_{in}$. Without the polarization $\langle S_z \rangle = 0$ and $P = 0$, the absorption of pumping light is the strongest. The minimum output voltage satisfies $\ln V_{min} = \ln V_{max} - OD$.

So, we can calculate the electron polarization P with the output of the detector,

$$P = \frac{\ln V_{out} - \ln V_{min}}{\ln V_{max} - \ln V_{min}}, \tag{7}$$

where P refers to the average polarization inside the pumping beam, the *OD* is calibrated with $\ln V_{max} - \ln V_{min}$. When $V_{max} \ll V_{min}^{(1+1/P)}$, there is a nearly linear relationship between V

and P. In the later measurement of time constants τ_{MROP} and τ_{OPMR}, we suppose that V and P have a similar decay time.

As we know, a fully polarized state cannot be achieved experimentally. Since the incident light with large detuning hardly interacts with the atomic ensemble, we simulate the attenuation without absorption in the case of a fully polarized cell by detuning the frequency of the incident light to about 40 GHz. The transmitted voltage is denoted by V_{max}. The absorption of light in the case of an unpolarized cell is simulated by using the resonant linearly polarized light. We determined V_{min} by adjusting the quarter-wave plate in front of the cell and searching for the minimum transmitted voltage. The transmitted voltage is denoted by V_{min}. The blue line and the red line in Fig. 3 are V_{max} and V_{min} calibrated by simulation when the optical power is 110 μW, respectively. They are the statistical average values in about 5 s sampling time.

Figure 3 shows the calibrated results of the polarization. When circularly polarized light passes through the rubidium cell, the transmitted signal changes periodically with the resonant RF pulse. The transmitted voltage signal can be calibrated into the polarization of the cell by using Eq. (7). The dashed lines show the exact values of the polarization of the rubidium atom system at optical pumping steady state (corresponding to RF OFF) and magnetic resonance steady state (corresponding to RF ON), which are 0.615 and 0.393, respectively. The polarization difference ΔP duo to RF magnetic resonance is 0.222. The aperture diameter is 1 mm, the optical pumping power is 110 μW, and the current amplitude of RF coils is 1.8 mA.

Then, the dependence of polarization difference ΔP between two steady states on optical pumping power is obtained. As shown in Fig. 4, ΔP tends to increase first and then decrease with a gradual increase in pumping optical power. With a moderate pumping power P_0 of about 70 μW, the maximum of ΔP is attained.

Based on Eqs. (5) and (6), $\Delta P = P_{OP} - P_{MR}$ due to the RF field can be expressed as

$$\Delta P = \frac{2R_{rf}R_{op}}{R_{op}^2 + 2(R_{rf} + R_{rel})R_{op} + R_{rel}(R_{rel} + 2R_{rf})}. \tag{8}$$

Its partial derivative $\partial(\Delta P)/\partial R_{op}$ can be shown as

$$\frac{-2R_{rf}R_{op}^2 + 2R_{rf}R_{rel}(R_{rel} + 2R_{rf})}{[R_{op}^2 + 2(R_{rf} + R_{rel})R_{op} + R_{rel}(R_{rel} + 2R_{rf})]^2}.$$

Setting $\partial(\Delta P)/\partial R_{op} = 0$, the pumping rate of P_0 corresponding to the maximum of ΔP is

$$R_{op}(P_0) = \sqrt{R_{rel}(R_{rel} + 2R_{rf})}. \tag{9}$$

It indicates that P_0 depends on R_{rf} and R_{rel}.

V. TRANSIENT PROCESS ANALYSIS OF SPIN POLARIZATION

As is shown in Fig. 3, by monitoring the intensity of the transmitted pumping laser, the transient response of the atomic spin ensemble is investigated during which the polarization of the atom ensemble is switched periodically by an RF pulse. In this way, two time constants of the transient process are studied. The decay time of absorption τ_{MROP} from magnetic resonance steady state to optical pumping steady state is measured experimentally under

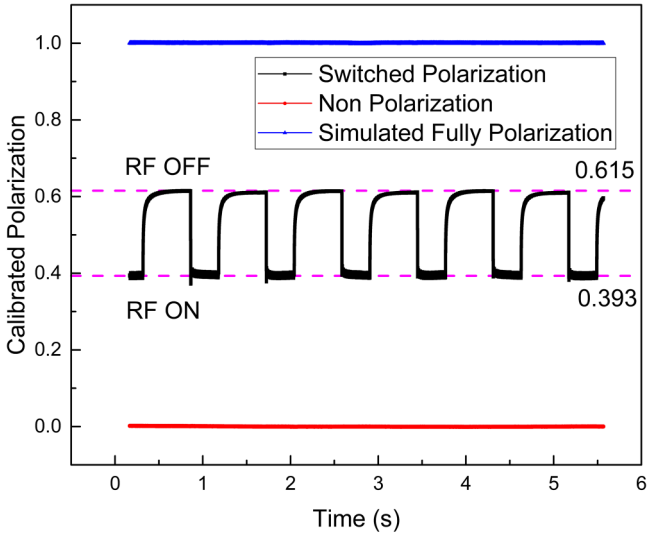

FIG. 3. The calibrated polarization of the Rubidium ensemble with a 110 μW circularly polarized pumping laser and a switched resonant RF field.

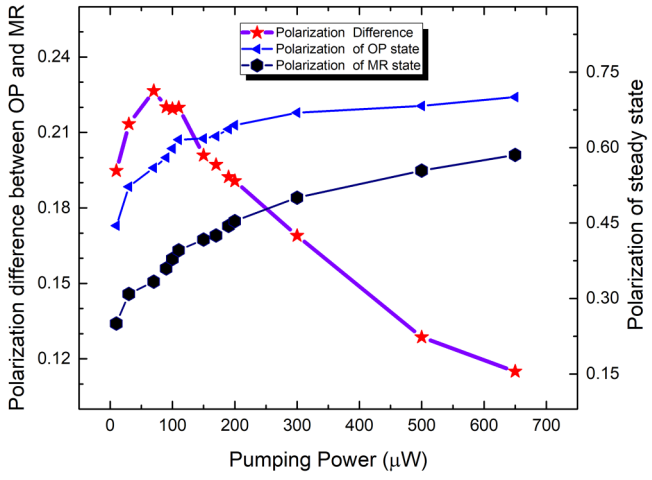

FIG. 4. The polarization of optical pumping and magnetic resonance steady states, as well as the polarization difference with respect to the pumping power, where the current amplitude of RF coils is 1.8 mA and the aperture is 1 mm in diameter.

different pumping power, as well as the decay of transmission τ_{OPMR} from optical pumping steady state to magnetic resonance steady state under different RF driving.

Figure 5 depicts the relation between the decay time τ_{MROP} and the pumping power with a certain RF driving rate. The applied current amplitude of RF coils is 1.8 mA for the improved signal-to-noise ratio. The incident pumping power is changed to observe and collect the transmitted signal, the same as in Fig. 3. Combined with Eq. (4), the decay time is attained by exponential fitting on the rising edge of the transmitted signal. In order to avoid the accidental error of a single measurement, six cycles are collected at each pumping power. As shown in Fig. 5, the decay time is the average value of those six decays of rising edges. The error bar of six repeated measures is also shown in the figure. The experiments are carried out with apertures of 6, 3, and 1 mm in diameter, as is shown in Figs. 5(a)–5(c), respectively.

In combination with Eq. (4), the decay time is $\tau_{MROP} = 1/(R_{op} + R_{rel})$. When a resonant light interacts with the atomic system, the electric dipole transition probability is proportional to the light intensity. Therefore, with the fitting function $y = c + 1/(ax + b)$, the scale factor of R_{op} to pumping power and R_{rel} are given under different pumping beam sizes, as shown in Table I. The black short dashed line in Fig. 5 is the fitting curve.

Figure 6 shows the dependence of τ_{OPMR} on the current amplitude of RF coils, where the beam diameter is 1 mm. Similar to Fig. 3, six falling edges are collected under each RF driving rate. The average value of those six decay time constants of falling edges is given, in addition to the error bar. The pumping powers of Figs. 6(a) and 6(b) are 100 and 10 μW, respectively.

In combination with Eq. (5), $\tau_{OPMR} = 1/(R_{op} + R_{rel} + 2R_{rf})$. When a resonant magnetic field interacts with the atomic system, the magnetic dipole transition probability is proportional to the square of Rabi frequency. As we know, the Rabi frequency of the magnetic resonance is γB_1, where γ is the gyromagnetic ratio of rubidium 85 and the RF field is $2B_1\cos(\omega t)$. With the fitting model $y = c + 1/(2ax^2 + b)$, the scale factor of R_{rf} to the square of the current amplitude of RF coils is obtained, as shown in Table II. The red short dashed line in Fig. 6 is the fitting curve. On the condition that the pumping power is certain, the stronger the RF field, the stronger the absorption signal, which depends on the AC current amplitude of RF coils. In addition, if the current amplitude is greater than 1.8 mA, Rabi oscillation can be observed by switching the RF field, which has a similar signal to Refs. 34 and 35 by switching B_0, but in this paper, that is not our topic. Therefore, the upper limit of current amplitude is 1.8 mA.

In brief, we demonstrated a method to obtain R_{rel} and two scale factors on R_{op}, R_{rf}, which are important parameters for theoretical and experimental analysis. In fact, the magnetic field spatial gradient, the drift of the main magnetic field, and the residual transverse magnetic will disturb or destroy the magnetic resonance condition. We believe that an additional magnetic shield will improve the measurements dramatically.

TABLE I. The scale factor of R_{op} and rate of relaxation vs pumping aperture.

The aperture (mm)	1	3	6
Scale factor of R_{op} ($10^{-3} \times s^{-1}/\mu W$)	192	173	207
Rate of relaxation (s^{-1})	21.6	23.8	23.3

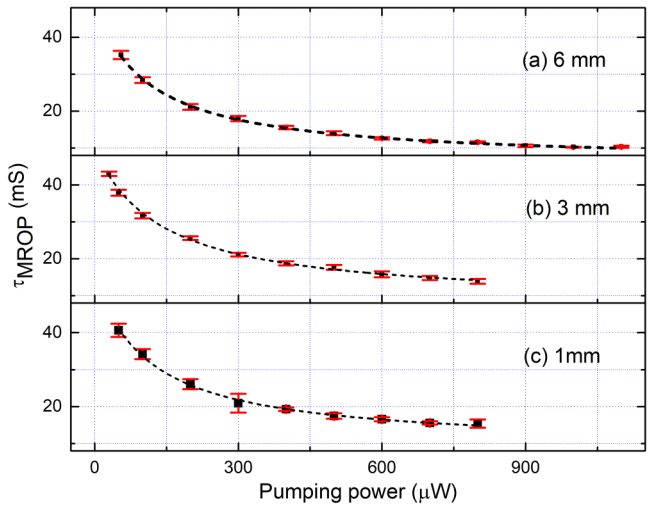

FIG. 5. The decay time of spin system from magnetic resonance steady state to optical pumping steady state vs the pumping power. The current amplitude of RF coils is 1.8 mA. The aperture is (a) 6, (b) 3, and (c) 1 mm in diameter.

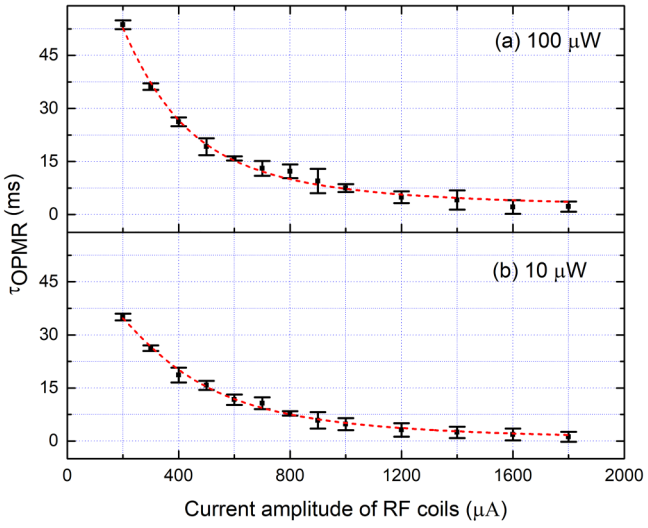

FIG. 6. Relationship between decay time constant τ_{OPMR} of spin ensemble from optical pumping steady state to magnetic resonance steady state and RF current amplitude in experiments, and the coefficient factor is 52 nT/mA. The apertures are 1 mm in diameter, where the pumping power is (a) 100 and (b) 10 μW.

TABLE II. The scale factor of the rate of RF transition.

Pumping power (μW)	10	100
Scale factor ($10^{-5} \times s^{-1}/(\mu A)^2$)	8.6	8.5

VI. CONCLUSION

We have studied the time responses of a spin system under a resonant RF pulse controlling based on monitoring the pumping light absorption. The spin evolution and spin relaxation are stimulated by the RF pulse. When the RF magnetic field is switched on and off periodically, the spin system will evolve between the optical pumping steady state and the magnetic resonance steady state. In the steady-state analysis, the optimal pumping rate or power value corresponding to the maximum polarization difference is obtained. As to the transient response, the decay time constants τ_{MROP} and τ_{OPMR} are measured experimentally. The intensity dependence of pumping laser on τ_{MROP} and the RF driving field on τ_{OPMR} are investigated. According to the two scale factors obtained by fitting, we can calculate R_{op} and R_{rf} corresponding to a certain optical pumping power and an RF magnetic field. The results could be beneficial to the application based on the spin polarized atomic ensemble.

ACKNOWLEDGMENTS

This work was suppoted by the National key R&D Program of China (Grant No. 2017YFA0304502) and the National Natural Science Foundation of China (NNSFC) (Grant No. 11974226). The authors thank Dr. Nan Zhao for helpful discussions.

AUTHOR DECLARATIONS

Conflict of Interest

The authors have no conflicts to disclose.

DATA AVAILABILITY

The data that support the findings of this study are available from the corresponding author upon reasonable request.

REFERENCES

[1]C. L. Degen, F. Reinhard, and P. Cappellaro, Rev. Mod. Phys. **89**, 035002 (2017).
[2]A. D. Ludlow, M. M. Boyd, J. Ye, E. Peik, and P. O. Schmidt, Rev. Mod. Phys. **87**, 637 (2015).
[3]D. Budker and M. Romalis, Nat. Phys. **3**, 227 (2007).
[4]H. B. Dang, A. C. Maloof, and M. V. Romalis, Appl. Phys. Lett. **97**, 151110 (2010).
[5]D. Sheng, A. Kabcenell, and M. V. Romalis, Phys. Rev. Lett. **113**, 163002 (2014).
[6]C. Johnson, P. D. D. Schwindt, and M. Weisend, Appl. Phys. Lett. **97**, 243703 (2010).
[7]H. Xia, A.-A. Baranga, D. Hoffman, and M. V. Romalis, Appl. Phys. Lett. **89**, 211104 (2006).
[8]Y. J. Kim, I. Savukov, and S. Newman, Appl. Phys. Lett. **114**, 143702 (2019).
[9]G. Bison, N. Castagna, A. Hofer, P. Knowles, J.-L. Schenker, M. Kasprzak, H. Saudan, and A. Weis, Appl. Phys. Lett. **95**, 173701 (2009).
[10]P. Bevington, R. Gartman, and W. Chalupczak, J. Appl. Phys. **125**, 094503 (2019).
[11]M. A. Rosenberry and T. E. Chupp, Phys. Rev. Lett. **86**, 22 (2001).
[12]M. Jiang, H. Su, A. Garcon, X. Peng, and D. Budker, Nat. Phys. **17**, 1402–1407 (2021).
[13]H. Su, Y. Wang, M. Jiang, W. Ji, P. Fadeev, D. Hu, X. Peng, and D. Budker, Sci. Adv. **7**, eabi9535 (2021).
[14]T. R. Gentile, P. J. Nacher, B. Saam, and T. G. Walker, Rev. Mod. Phys. **89**, 045004 (2017).
[15]T. G.Walker and W. Happer, Rev. Mod. Phys. **69**, 629 (1997).
[16]M. S. Albert, G. D. Cates, B. Driehuys, W. Happer, B. Saam, C. S. Springer, Jr., and A. Wishnia, Nature **370**, 199 (1994).
[17]T. W. Kornack, R. K. Ghosh, and M. V. Romalis, Phys. Rev. Lett. **95**, 230801 (2005).
[18]C. Beecham, S. Boag, C. Frost, T. McKetterick, J. Stewart, K. Andersen, P. Bentley, and D. Jullien, Physica B **406**, 2429 (2011).
[19]A. Kastler, J. Opt. Soc. Am. **47**, 460 (1957).
[20]W. Happer, Rev. Mod. Phys. **44**, 169 (1972).
[21]H. G. Robinson and C. E. Johnson, Appl. Phys. Lett. **40**, 771 (1982).
[22]M. A. Bouchiat and J. Brossel, Phys. Rev. J. Arch. **147**, 41 (1966).
[23]K. F. Zhao, M. Schaden, and Z. Wu, Phys. Rev. A **81**, 042903 (2010).
[24]S. J. Seltzer and M. V. Romalis, J. Appl. Phys. **106**, 114905 (2009).
[25]K. Zhang, H. Yang, A. Li, Y. Wang, and N. Zhao, Appl. Phys. Lett. **113**, 064101 (2018).
[26]R. Li, W. Quan, and J. Fang, IEEE Photon. J. **9**, 4502708 (2017).
[27]S. J. Seltzer and M. V. Romalis, Appl. Phys. Lett. **85**, 4804 (2004).
[28]H. C. Huang, H. F. Dong, X. Y. Hu, L. Chen, and Y. Gao, Appl. Phys. Lett. **107**, 182403 (2015).
[29]R. G. Brewer and R. L. Shoemaker, Phys. Rev. A **6**, 2001 (1972).
[30]E. L. Hahn, Phys. Rev. J. Arch. **80**, 580 (1950).
[31]R. Shaham, O. Katz, and O. Firstenberg, Phys. Rev. A **102**, 012822 (2020).
[32]J. Zhao, M. Ding, J. Lu, K. Yang, D. Ma, H. Yao, B. Han, and G. Liu, IEEE Trans. Instrum. Meas. **69**, 845 (2020).
[33]G. Bevilacqua, V. Biancalana, Y. Dancheva, A. Fregosi, and A. Vigilante, Appl. Phys. B **127**, 128 (2021).
[34]J. Tang, Y. Yin, Y. Zhai, B. Zhou, B. Han, H. Yang, and G. Liu, Opt. Express **29**, 8333 (2021).
[35]G. Jin, Y. Xu, and Z. Wang, Opt. Express **27**, 7087 (2019).